Automatic Liver segmentation Using Vector Field Convolution and Artificial Neural Network in MRI Images

Hassan Masoumi[1], Ahad Salimi[1], Hamidreza Sadeghi Madavani[2]
1- Department of engineering,Kazerun Branch, Islamic Azad University, Kazeron, Iran.
Email: H.masoumii@yahoo.com, Email: Ahadsalimi@yahoo.com
2- Department of engineering,Zarindasht Branch, Islamic Azad University, Zarindasht, Iran.
Email: Hamid_Madavni@yahoo.com

Received: December 2011 Revised: January 2012 Accepted: February 2012

ABSTRACT:
Accurate liver segmentation on Magnetic Resonance Images (MRI) is a challenging task especially at sites where surrounding tissues such as spleen and kidney have densities similar to that of the liver and lesions reside at the liver edges. The first and essential step for computer aided diagnosis (CAD) is the automatic liver segmentation that is still an open problem. Extensive research has been performed for liver segmentation; however it is still challenging to distinguish which algorithm produces more precise segmentation results to various medical images. In this paper, we have presented a new automatic system for liver segmentation in abdominal MRI images. Our method extracts liver regions based on several successive steps. The preprocessing stage is applied for image enhancement such as edge preserved and noise reduction. The proposed algorithm for liver segmentation is a combined algorithm which utilizes a contour algorithm with a Vector Field Convolution (VFC) field as its external force and perceptron neural network. By convolving the edge map generated from the image with the user-defined vector field kernel, VFC is calculated. We use trained neural networks to extract some features from liver region. The extracted features are used to find initial point for starting VFC algorithm. This system was applied to a series of test images to extract liver region. Experimental results showed the promise of the proposed algorithm.

KEYWORDS: Neural Network, VFC algorithm, Segmentation, Preprocessing, Sticks filter, Gaussian filter.

1. INTRODUCTION

Nowadays, imaging techniques such as Magnetic Resonance Imaging (MRI), Computed Tomography (CT) and Positron Emission Tomography (PET) are very pivotal in medical diagnosis. Hepatic MRI is a new diagnostic method which produces high quality images and is one of the standard instruments for diagnosis of liver pathologies such as cirrhosis, liver cancer and fulminant hepatic failure [1]. Such advances include rapid scanning, new sequences of volumes with a very high spatial resolution and more specific contrast for each type of lesion [2, 3].

Fast and suitable algorithms for segmentation play an important role in disease diagnosis, classification and quantitative description of various tissues and diagnosing liver tumors [4]. For example, in clinic surgery, one of the important and crucial steps is the accurate segmentation of liver in MRI images for automated liver perfusion analysis, which provides important information about the blood supply to the liver [5]. Accurate liver segmentation in abdominal MRI is a challenging issue since the grey level distribution of surrounding organs is not highly distinguishable. Therefore, the boundary regions between liver and adjacent tissues generally have uniform intensity distributions, which often lead to over segmentation of the liver. Additionally inner vascular inside the liver commonly leads to segmentation leakage [6]. So far, many researches have been performed for liver segmentation in CT images. However, only a few of them handle MRI images. The first and foremost reason is that abdominal MRI images are more artifacts affected. Also, they have a low gradient response, which makes accurate liver segmentation very difficult [7].

Zhang et al. proposed an automatic liver segmentation method in CT images based on a Statistical Shape Model (SSM) integrated with an optimal-surface-detection strategy [8]. The method included three steps; first, the localization of the average liver shape model was used in a test CT volume via 3-D generalized Hough transform. Then, subspace initialization of the SSM was performed by intensity and gradient profile. Finally, the shape model was deformed to adapt to liver contour through an optimal-surface-detection approach based on graph theory. Badakhshannoory et al. proposed a model-based validation scheme for organ segmentation in CT

scan volumes [9]. In this method, instead of using the organ's prior information directly in the segmentation process, the knowledge of the organ was utilized to validate a large number of potential segmentation outcomes that are generated by a generic segmentation process. For this purpose, an organ space was generated based on the principal component analysis approach. The method was employed for the 3-D segmentation of human kidney and liver in CT scan volumes.

Lamecker et al. evaluated the 3D statistical shape model for liver segmentation in CT images [10]. In this method, a geometric approach based on minimizing the distortion of the correspondence mapping between two different surfaces was utilized. For the adaption of the shape model to the image data a profile model based on the grey value appearance of the liver, and its surrounding tissues in contrast enhanced CT data was developed.

The authors of reference [11] proposed an automatic liver segmentation system by combining several phases of the contrast-enhanced CT images. The method employed region-growing algorithm facilitated by pre- and post-processing functions, which incorporate anatomical and multi-phase information to eliminate over- and under-segmentation. Foruzan et al. employed a knowledge-based technique for liver segmentation in CT images [12]. In order to estimate the liver initial boundary, the method utilized a technique based on anatomical knowledge of liver and its surrounding tissues. Furthermore, a multi-step heuristic technique was employed to segment liver from other tissues in multi-slice CT images.

In [13] an automatic liver segmentation algorithm for volume measurement in CT image was presented. The algorithm analyzed the intensity distribution of several abdominal CT samples to exploit a priori knowledge such as CT numbers (Hounsfield number) and location of the liver to identify coherent regions that correspond to the liver. In this method, recursive morphological filter with region-labeling and clustering were utilized to detect the search range and generate the initial liver contour. Then, liver contour was deformed using the labeling-based search algorithm and finally volume measurement was performed on the segmented liver regions.

Gao et al. employed an automatic liver segmentation system for three-dimensional visualization of CT data. They combined domain knowledge with the analysis of a global histogram, morphological operation and the parametrically deformable contour model [14]. Boundaries of the thresholded liver volume were modified section by section exploiting information from adjacent sections. These boundaries were refined by the optimization of the parametrically deformable contour model. Finally, volume rendered image was created by using the boundaries to exclude tissues outside the liver. The authors of reference [15] proposed a liver segmentation method using Gradient Vector Flow (GVF) snake in CT images. The method utilized a snake algorithm with a GVF field as its external force. To improve the performance of the GVF snake in the segmentation of the liver contour, an edge map was obtained using Canny edge detector, followed by modifications using a liver template and a concavity removal algorithm. By using the modified edge map, for which unwanted edge points inside the liver were eliminated, the GVF field was computed, and an initial liver contour was formed. The snake algorithm was then applied to obtain the actual liver contour.

Bae et al. proposed an automatic liver segmentation system in CT images that automatically extract liver structure from abdominal CT scans using a priori information about liver morphology and some image-processing techniques [16]. Segmentation was performed sequentially image-by-image starting with a reference image in which the liver occupies almost the entire right half of the abdomen cross section. Image processing techniques included gray-level thresholding, Gaussian smoothing, and eight-point connectivity tracking. In this algorithm, the shape, size, and pixel density distribution of the liver were recorded for each CT image and used in the processing of other CT images. Extracted boundaries of the liver were also smoothed using mathematical morphology techniques and B-splines. The authors of reference [17] proposed a diagnostic system for CT liver image classification. The method finds the CT liver boundary and classifies liver diseases. The system includes a detect-before-extract (DBE) system which finds the liver boundary. Furthermore, a neural network based liver classifier is utilized to distinguish normal liver as well as two types of liver tumors including hepatoma and hemageoma. The DBE system employs the concept of the normalized fractional Brownian motion model to find an initial liver boundary and then uses a deformable contour model to precisely delineate the liver boundary.

The authors of reference [18] proposed a liver segmentation method from contrast-enhanced CT images. In this method, the two-step seeded region growing (SRG) onto level-set speed images was applied to define an initial liver boundary. The first SRG efficiently divides the CT image into a set of discrete objects based on the gradient information and connectivity. The second SRG detects the objects belonging to the liver based on a 2.5-dimensional shape propagation. The method also used level-set speed images for level-set propagation to detect the initial liver boundary. Finally, a rolling ball algorithm was applied to refine the liver boundary more accurately.Zhao et al. proposed a liver segmentation algorithm in CT images, where a thresholding method

was used to remove the ribs and spines in the input image [19]. Additionally, the initial liver region was segmented by using fuzzy C-means clustering algorithm and morphological reconstruction filtering. Then a multilayer perceptron neural network was employed for the segmentation.

The authors of [20] employed an automatic liver segmentation method that utilizes low-level features based on texture information in CT images. This method included four successive steps: first, the pixel-level texture extraction algorithm was applied. Second, liver probability images were generated by using a binary classification approach. Third, a split-and-merge algorithm was applied to detect the seed set with the highest probability area and finally, a region growing algorithm was iteratively applied to the seed set in order to refine the liver boundary and obtain the final segmentation results. Moreover, the results were compared with different texture extraction methods such as Gabor filters and Markov random fields and co-occurrence matrices [21]. The authors of [22] proposed an automatic liver segmentation in abdominal CT images. At first, roughly liver tissue is distinguished by using a statistical model-based approach. It is followed by applying force-driven optimized active contour (snake) [23, 24] in order to obtain a smoother and finer liver contour.

Different algorithms have also been proposed for liver segmentation in MRI images. Chen et al. employed a multiple-initialization LSM algorithm to overcome the leakage and over-segmentation problems in liver segmentation from MRI images [5]. They first evolved the multiple-initialization curves separately using a fast marching method and LSMs, which were then combined with a convex hull algorithm to obtain a rough liver contour. Finally, the contour was evolved again using global level set smoothing algorithm to determine the precise liver boundary. The authors of [25], proposed a liver perfusion analysis based on active contours and Chamfer Matching (CM) [26, 27] that were employed for liver segmentation and aligning the slices in MRI series respectively. To apply CM, a prior liver shape image was employed to help liver shape extraction as well as removing artifacts. Gloger et al. proposed a three-step liver segmentation method using LDA-based probability maps for multiple contrast MR images [28]. The method is based on a modified region growing approach and thresholding algorithm. In this method, all available MR channel information of different weightings was used to formulate liver tissue and position probabilities in a probabilistic framework. The method utilized a multiclass linear discriminant analysis to generate probability maps for the segmentation. Finally, characteristic prior knowledge was incorporated to improve the segmentation results.

Yuan et al. proposed an automatic liver segmentation algorithm based on fast marching and improved fuzzy clustering methods in abdominal MRI images [6]. This method includes four successive steps. First, fast marching method and convex hull algorithm were applied to roughly extract the liver's boundary and topology. This step provides a basic estimation for the subsequent calculations. Second, an improved fuzzy clustering method, combined with a multiple cycles processing, was designed to refine the segmentation result. Third, based on the segmentation results, the liver is visualized by Marching Cube (MC) method. Middleton et al. proposed MRI segmentation algorithm based on the combination of neural networks and active contour models [29]. In this method, a perceptron neural network was trained to classify each image pixel as either a boundary or a non-boundary. Then, the resultant binary image was utilized to define the external energy function for the snake. Consequently, by minimizing snake energy the final result was obtained.

In this paper, we have proposed a new method for automatic liver segmentation in abdominal MRI images. The algorithm is fully automatic and contains several stages, including preprocessing, automatic initial point generation and segmentation. The preprocessing stage is applied for enhancing main edges of the image regions while removing image noise. Then the neural networks are used in initial point detecting step to extract some features of liver region and finally the boundary of liver is segmented by using VFC algorithm [30]. Although, active contour or snakes have been widely used in medical image segmentation, limited capture range, noise sensitivity, and poor convergence to concavities are typical roadblocks to consistent performance. To address these problems, a novel external force called VFC are proposed which minimize specific snake problems and enhance convergence speed. This external force field is calculated by convolving a vector field kernel with the edge map derived from the gray-level or binary image. Snakes that use the VFC external force are termed VFC snakes. Similar to the GVF approach, instead of being formulated using the standard energy minimization framework, VFC snakes are constructed by way of a force balance condition. Advantages of VFC snakes over GVF are demonstrated by comparison with it in section 3.

The reminder of the paper is as follows. Section 2 describes the proposed algorithm for liver segmentation. Section 3 represents the experimental results, and finally, we conclude the paper in section 4.

2. AUTOMATIC LIVER SEGMENTATION SYSTEM

Figure 1 shows the block scheme of the proposed system. The proposed system consists of different stages, including preprocessing, and liver extraction. In the preprocessing stage, we apply two consecutive processes to input image, including sticks filter and Gaussian filtering.

The liver extraction algorithm includes feature extraction using neural network and liver region determination using VFC algorithm. Multilayer perceptron neural networks are trained and used to extract some features from MRI images which used to find initial point for starting VFC algorithm automatically. For rapid segmentation and interpretation of different samples, the liver region is finally extracted using VFC algorithm. This algorithm was also extended to segment the liver in a slice-by-slice fashion, where the result of the preceding slice constrained the segmentation of the next slice.

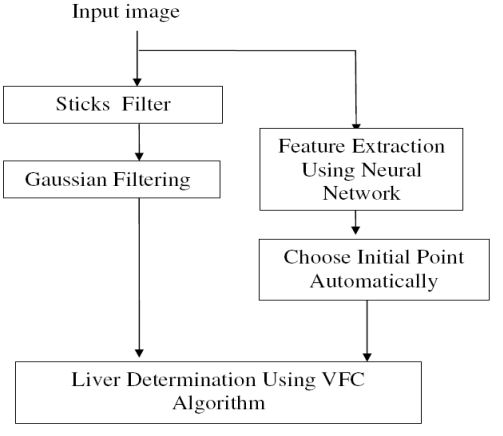

Fig. 1. Block diagram of the proposed system

2.1. Preprocessing

Most of abdominal MRI images are noisy and the edges of objects are not clear enough. Hence the usual segmentation algorithms, leads to not recognizing main edges as well as extracting additional boundaries. To handle this problem, we applied preprocessing stage to the input image before applying the main segmentation stage [31]. In this paper, preprocessing is the combination of sticks filter and Gaussian filtering which are applied to prevent the generation of insignificant regions in the main segmentation stage.

Sticks filter is a very powerful tool to enhance the boundaries and the image contrast in medical images, especially in ultrasound images [32]. It is possible to significantly reduce noise and improve edge information, making them more suitable for edge detection. Consider a small square of size N * N around each pixel in the image that N is the stick's length in pixels. There are 2N- 2 possible orientations lines that pass through the central pixel; with each line having N pixels. The sum of pixel values along each line segment is calculated. The largest sum of segments is put in center pixel of N*N sub matrix in the image. This step is repeated for all pixels. Figure 2 illustrates the eight possible line segments presented in a small 5*5 neighborhood. Output shows that noise is decreased, while the contrast at the edge is increased.

In the second step of preprocessing, we then apply Gaussian filter. The kernel for Gaussian filter is calculated using Eq. 1 and applied to the output of previous step i.e. *Is* to produce GFI as follows:

$$G(x,y)=\frac{1}{2\pi\sigma^2}\exp\left[\frac{(-x^2-y^2)}{2\sigma^2}\right] \quad (1)$$

$$GFI = Is * G \quad (2)$$

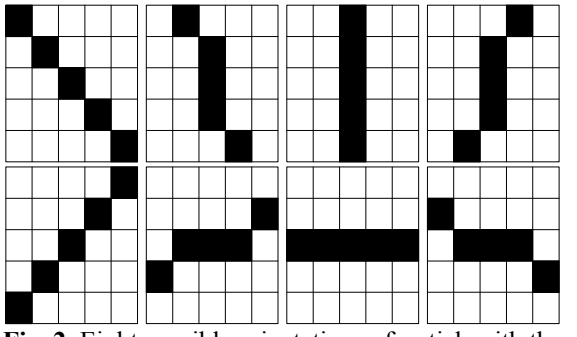

Fig. 2. Eight possible orientations of a stick with the length of five

2.2. Automatic Initial Point Generation

VFC segmentation method normally starts with a single pixel called initial point. In our method, the initial point location is automatically generated by the multilayer perceptron neural network configuration. To generate the initial point, we used two shapes based on liver which are the center of masses in vertical and horizontal directions. Two different neural networks are utilized which are trained individually for the estimation of these features. The structure of these networks which are trained by Back Propagation Algorithm (BPA) [33] is shown in figure 3. To make the features more robust against the size variation of the input image we normalize the necessary features using the input image dimensions. To obtain necessary inputs for neural networks, the input image is normalized to the constant size of $m \times n$ and average pixel values are calculated for different rows of the normalized images. The result of averaging is a vector of size $m \times 1$ for each image which is used for the input of neural network. We used three layer neural networks with m neurons in input layer and one neuron in output layer. The neuron of output layer shows the extracted feature which its value during the

training stage is determined by manually segmenting the liver area in the input image. Finally center of masses for liver area in vertical and horizontal directions are given respectively by:

$$x = CMx \times R \tag{3}$$

$$y = CMy \times C \tag{4}$$

where *CMx and CMy* are normalized center of masses for liver area in vertical and horizontal directions respectively which are extracted by neural networks . *R* and *C* are the height and width of input image. Coordinates x and y are used as an initial point location for VFC segmentation method on each input image.

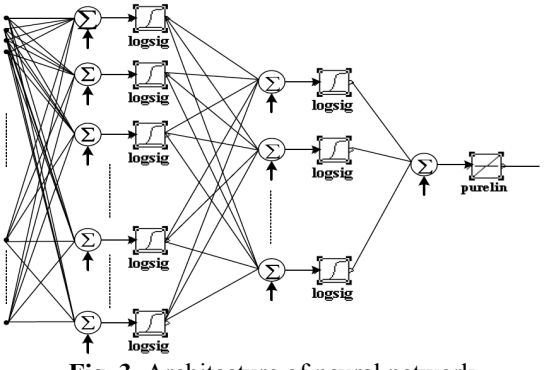

Fig. 3. Architecture of neural network

2.3. VFC Segmentation Method

In this stage, we extract the liver region using a snake algorithm with a vector flow convolution (VFC) field as its external force. Active contours or snakes are curves that move within images to find object boundaries. The curve is represented by:

$$X(S) = [x(s), y(s)] \qquad s \in [0,1] \tag{5}$$

It also deforms through the image to minimize the energy function [34]:

$$E_{AC} = \int_0^1 [\frac{1}{2}(\alpha \left|X'(s)\right|^2 + \beta \left|X''(s)\right|^2) + E_{ext}(X(s))]ds \tag{6}$$

where α and β are parameters representing the degree of the smoothness and tautness of the contour respectively. X'(*s*) and X''(*s*) are the first and second derivatives of X(*s*) with respect to *s*. The external energy E_{ext} is derived from the image. As object boundaries are usually of high gradient in the image *I* (*x*, *y*), a typical example of external energy for seeking the edges is given as:

$$E_{ext}(x, y) = -\left|\nabla I(x, y)\right|^2 \tag{7}$$

where ∇ denotes the gradient operator. The external force F_{ext} is derived from external energy and defined so as to attract the snake to strong edges:

$$F_{ext}(X) = -\nabla E_{ext}(X) \tag{8}$$

To minimize Eq.6, the contour must satisfy the Euler equation:

$$\alpha x''(s) - \beta x''''(s) - \nabla E_{ext} = 0 \tag{9}$$

The gradient vector flow (GVF) is the vector field proposed by Xu et.al [36] as a new external force for snakes to solve the drawbacks of traditional snakes. The GVF field is the vector field:

$$v(x, y) = [u(x, y), v(x, y)] \tag{10}$$

That minimizes the energy function:

$$E_{GVF} = \iint \mu(u_x^2 + u_y^2 + v_x^2 + v_y^2) + \left|\nabla f\right|^2 \left|v - \nabla f\right|^2 \partial x \partial y \tag{11}$$

where $f = -E_{ext}$ is an edge map derived from the image and μ is a parameter controlling the degree of smoothness of the vector field. By replacing the external force F_{ext} by the GVF field **v**, a solution for GVF snake can be obtained. The external energy E_{ext} is derived from the image and set to small values at features of interest. As object boundaries are usually of high gradient in the image *I* (*x*, *y*), a typical example of external energy for seeking the edges is given as

$$E_{ext}(x, y) = -\left|\nabla[G_\sigma(x, y) * I(x, y)]\right|^2 \tag{12}$$

where $G_\sigma(x, y)$ a 2D Gaussian function with standard deviation σ. * is denotes linear convolution and ∇ denotes the gradient operator. As mentioned in [15], although the GVF field improved the external force to accommodate a large capture range and to enable faithful representation of curve concavities in liver segmentation, there are some disadvantages, such as the sensitivity to the parameters, the obscure relationship between the capture range and the parameters, the capture range sensitivity to noise, especially impulse noise, and expensive computational cost. Therefore, in this paper we used a new external force called VFC that solved the problems of GVF and also has better robustness to noise and initialization, flexibility of changing the force field, and reduced computational cost. Vector field convolution snakes are active contours using the VFC field as the external force.

First of all, a vector field kernel ($K(x, y) = [s(x, y), t(x, y)]$) is defined in which all the vectors point to the origin:

where *m*(*x*, *y*) is the magnitude of the vector at (*x*,*y*) and n(*x*, *y*) is the unit vector pointing to the origin:

$$K(x, y) = m(x, y)n(x, y) \tag{13}$$

where *m*(*x*, *y*) is the magnitude of the vector at (*x*,*y*) and n(*x*, *y*) is the unit vector pointing to the origin:

$$n(x, y) = [\frac{-x}{r}, \frac{-y}{r}] \tag{14}$$

where $r = \sqrt{x^2 + y^2}$ is the distance from the origin, except that n(0,0) = [0,0] at the origin. A desirable external force should have an important property: a free particle placed in the field should be able to move to the features of interest, such as edges. If the origin is considered as the feature of interest, this vector field possesses this desirable property.

The vector field convolution (VFC) external force $v(x, y) = [u(x, y), v(x, y)]$ is given by calculating the convolution of the vector field kernel k(x, *y*) and the edge map *f*(*x*,*y*) generated from the image *I* (*x*, *y*):

$$v(x,y) = f(x,y) * K(x,y) = [f(x,y) * s(x,y), f(x,y) * t(x,y)] \quad (15)$$

where * denotes convolution. Since edge map *f* (x, *y*) is larger near the image edges, edges contribute more to the VFC than homogeneous regions. Therefore, the VFC external force can move free particles to the edges. The VFC field is strongly dependent on the magnitude of the vector field kernel *m*(*x*, *y*). By considering the fact that the influence from the feature of interest should be less as the particles are further away, the magnitude should be a decreasing function of distance from the origin. In this paper, the type of magnitude function, given as:

$$m(x, y) = (r + \varepsilon)^{-\gamma} \quad (16)$$

where γ is positive parameter to control the decrease, ε is a small positive constant to prevent division by zero at the origin. m (x , y) is inspired by Newton's law of universal gravitation in physics which is proposed in [36].

2.4. Segmentation of other slice

As mentioned before, the initial point location is automatically generated by the artificial neural network. It is only performed in the first slice of the abdominal MRI images and not all the slices of them need to use the methods mentioned above to obtain an initial point location. After liver extraction in the first slice, the centers of masses in vertical and horizontal directions of the liver region are saved. For other slice, the initial point location can be obtained from the centers of masses in vertical and horizontal directions of previous neighbor slice. Then VFC algorithm is applied to segment the current slice. So, the segmentation of the liver is automatically performed in all slices.

3. EXPERIMENTS

The proposed algorithm was implemented using a MATLAB program and tested using the collected dataset. Our dataset includes 113 abdominal MRI images with the size of 256×256 pixels, which were obtained from Imaging Center of Karaj, Iran. MRI images were scanned by a GE Medical Systems and have the slice thickness of 5.0mm, repetition time of 3.5 second, echo time of 1.2 second, field of magnetic1.5 tesla, and flip angle of 55 degree. In preprocessing, we used N=7 and 3×3 window in sticks filter and Gaussian filtering respectively. Figure 4 shows a typical abdominal MRI image and the effect of preprocessing stage. As it is shown in the figure, the contrast at the edge is increased while noise is reduced.

We also used two three-layer neural networks for the extraction of shape based features. To train the neural networks the MRI images are normalized to the fixed size of 100×100. Therefore, neural networks have 100 neurons in the first layer. We also used 10 neurons in the second layer experimentally, and one neuron in the third layer. Sigmoid activation function is used in the first and second layer, and linear function is used in the third layer. The neural networks were trained in 550000 iterations and learning rate of α = 0.001. Selection of this learning rate makes the neural network training time to increase, however the obtained weights give rise to higher accuracy. In this paper, 40% of images are randomly selected for the training of the neural networks. Table 1 shows the value of extracted features for 20 randomly selected test images obtained using the trained neural networks and manually. Comparing the value of table 1 shows the efficiency of training stage.

Figure 5 shows the result of segmentation using the proposed algorithm in several stages. The VFC algorithm is performed at maximum 300 iterations. α , β and γ are also (-4), (-11) and 2.52 respectability which are completely experimental. Figure 6 also demonstrates the result of segmentation using the proposed algorithm for 8 randomly slices which are performed automatically.

To compare the efficiency of the proposed algorithm with those of another method; we also implemented the method presented in reference [15] which is based on GVF method. This method has high calculation burden. To calculate accuracy of segmentation and compare the results of two methods we used the following equation:

$$ACC = \frac{N(A \cap B)}{N(A \cup B)} \quad (17)$$

where the A is the area of liver region extracted manually by an expert, B is the area of the liver extracted using the algorithm, $N(A \cap B)$ is the number of pixels for the intersection of two areas A and B and $N(A \cup B)$ is the number of pixel for the union of two areas A and B. For the best case, when the extracted area by algorithm is the same as area extracted manually, the ACC would be 1. In table 2 the accuracy of the proposed system is compared with GVF method for 20 randomly selected MRIs. We used the same preprocessing in two methods. The average accuracy for all test images is 0.9411 for the proposed algorithm and 0.9179 for GVF algorithm.

We also compare the time of calculation in table 3 with the method presented in reference [15] for 20 randomly selected MRIs. The average time of calculation for all test images is 37.12 seconds for the proposed algorithm and 48.23 seconds for GVF algorithm.

It is very important to note that the advantages of VFC snakes over GVF snakes are insensitivity to noise and initialization, flexibility of changing the capture range in a meaningful way, and reduced computational cost which demonstrates in results. However as the results show, the accuracy and time of calculation of the proposed algorithm is better than GVF algorithm. It is obvious that although the proposed algorithm is automatic, the results of the algorithm are more satisfactory than semi-automatic approaches which require human interaction. In addition, our implementation reveals the proposed algorithm is faster than the GVF method due to using timer.

3.1. Generality of Algorithm

The proposed algorithm is applicable for segmenting other areas in different medical imaging with some minor changes. To find the initial point location, it is only necessary to retrain the neural networks for the new area. Then the new area is segmented by VFC algorithm.

4. CONCLUSION

In this paper, we proposed a new automatic system for liver segmentation in abdominal MRI images which is the combination of preprocessing, obtaining an automatic initial point location and VFC segmentation method. According to our method, the problems of GVF and active contour segmentation method, sensitive to noise and automatic initial point location, are solved. Additionally preprocessing steps was utilized to prepare abdominal MRI images for segmentation. Also, we introduced an approach to obtain an automatic initial point location using perceptron neural network. We compared the results with that of another method and results showed the efficiency of the proposed method. The proposed algorithm has good capability for the segmentation of other regions in medical imaging. For future work we are going to focus on new and more effective methods for the measurement of liver volume in abdominal MRI images.

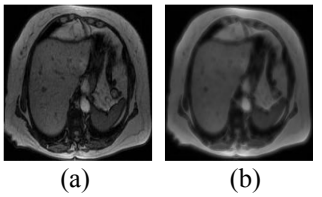

(a) (b)

Fig. 4. The effect of preprocessing stage (a) original image (b) result of preprocessing.

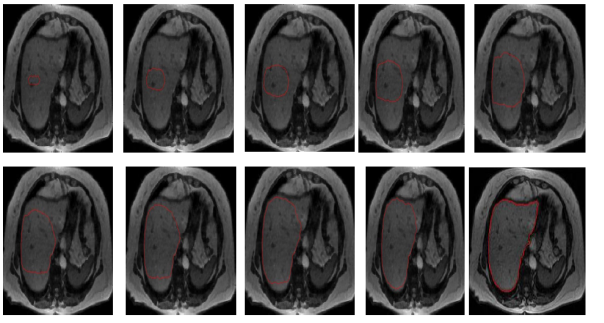

Fig. 5. Result of segmentation using VFC algorithm at maximum 300 iterations

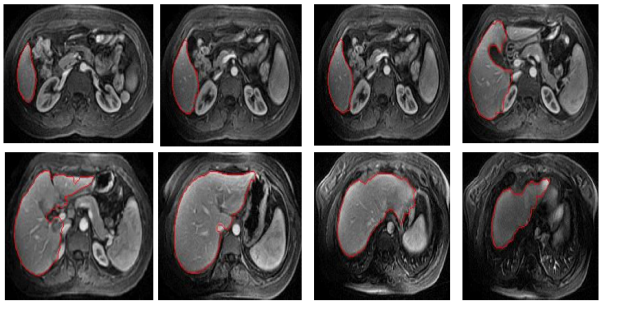

Fig. 6. Result of segmentation using proposed algorithm for 8 randomly slices

Table 1. The calculated features for 20 randomly selected images using neural network and manually

Test images	Calculated Features Using Trained Neural Networks		Calculated Features Manually	
	CM_x	CM_y	CM_x	CM_y
1	0.4401	0.3147	0.4882	0.3405
2	0.4761	0.3156	0.4772	0.3170
3	0.4557	0.2417	0.4763	0.3050
4	0.4113	0.3383	0.4997	0.3000
5	0.4343	0.3608	0.3968	0.3055
6	0.4266	0.3221	0.4762	0.3150
7	0.4252	0.3463	0.3809	0.3762
8	0.4603	0.2879	0.5246	0.3368
9	0.4713	0.3197	0.4326	0.3205
10	0.4514	0.3248	0.3996	0.3649
11	0.4779	0.2801	0.5060	0.3170
12	0.4733	0.3694	0.4495	0.2896
13	0.4349	0.3147	0.4296	0.3155
14	0.4359	0.3688	0.3917	0.3783
15	0.4776	0.2711	0.4846	0.3410
16	0.4462	0.3222	0.5046	0.2969
17	0.4842	0.2869	0.4836	0.3148
18	0.3769	0.3149	0.3635	0.3615
19	0.4914	0.3681	0.4656	0.3721
20	0.4628	0.2499	0.4308	0.2983

Table 2. Accuracy of GVF and proposed method for liver area extraction

Test Images	Method	
	Proposed Method	GVF
1	0.9415	0.9003
2	0.9411	0.9037
3	0.9183	0.8846
4	0.9591	0.9319
5	0.9006	0.8792
6	0.9573	0.9323
7	0.9345	0.8842
8	0.9311	0.9074
9	0.9149	0.8923
10	0.9440	0.9127
11	0.9199	0.8748
12	0.9401	0.9277
13	0.9219	0.9118
14	0.9053	0.8751
15	0.9288	0.9066
16	0.9216	0.8846
17	0.8838	0.8311
18	0.9569	0.9043
19	0.8931	0.8311
20	0.9233	0.8566

Table 3. The time of calculation OF GVF and proposed method for liver area extraction

TEST IMAGES	METHOD	
	TIME OF PROPOSED METHOD	TIME OF GVF
1	28.16	32.11
2	36.11	38.33
3	29.54	30.22
4	42.26	47.66
5	33.49	37.88
6	26.88	27.44
7	34.33	35.19
8	40.11	43.97
9	46.77	4.9.37
10	39.53	48.67
11	33.19	35.27
12	51.27	59.44
13	27.39	29.74
14	38.71	44.39
15	43.27	44.63
16	34.89	37.42
17	54.76	65.33
18	41.39	54.29
19	38.78	43.66
20	29.93	32.17

REFERENCES

[1] P. Capadelli, E. Casiraghi, G. Lombardi, **"Automatic liver segmentation from abdominal CT scans"**, *in: Proceedings of 14th International Conference on Image Analysis and Processing (ICIAP)*, 2007, pp.731-736.

[2] C. Bartolozzi, C.D. Pina, D. Cioni, L. Croceti, E. Batini, R. Lencioni, **"Magnetic Resonance: Focal Liver Lesions Detection"**, *Characterization, Ablation, Medical Radiology*, Springer, Berlin, 2005.

[3] C. Platero, J.M. Ponacela, P. Gonzalez, M.C. Tobary, J. Sanguino, G. Asensio, E. Santos, **"Liver segmentation for hepatic lesions detection and characterization"**, *in: Proceedings of 5th IEEE International Symposium on Biomedical Imaging*, 2008, pp. 13-16.

[4] V. Grau, A.U.J. Mewes, M. Alcaniz, R. Kikinis, S.K. Warfield, **"Improved watershed transform for medical image segmentation using prior information"**, *IEEE Trans. Med. Imag*., 23 (4) (2004) 447- 458.

[5] G. Chen, L. Gu, L. Qian, J. Xu, **"An improved level set for liver segmentation and perfusion analysis in MRIs"**, *IEEE Trans. Image Process.*, 30 (1) (2009) 94-103.

[6] Z. Yuan, Y. Wang, J. Yang, Y. Liu, **"A novel automatic liver segmentation technique for MR Images"**, *in: Proceedings of 3rd International Congress on Image and Signal Processing (CISP2010)*, 2010, pp. 1282-1286.

[7] S. Luo, Q. Hu, X. He, J. Li, J.S. Jin, M. Park, **"Automatic liver parenchyma segmentation from abdominal CT images using support vector machines"**, *in: Proceedings of International Conference on Complex Medical Engineering (ICME)*, 2009, pp.1-5.

[8] X. Zhang, J. Tian, K. Deng, Y. Wu, X. Li, **"Automatic liver segmentation using a statistical shape model with optimal surface detection"**, *IEEE Trans. Biomed*. Eng., 57 (10) (2010) 2622-2626.

[9] H. Badakhshannoory, P. Saeedi, **"A model-based validation scheme for organ segmentation in CT scan volumes"**, *IEEE Trans. Biomed. Eng.*, 58 (9) (2011) 2681–2693.

[10] H. Lamecker, T. Lange, M. Seebass, **"Segmentation of the liver using a 3d statistical shape model"**, *Technical Report, Zuse Institue*, Berlin (2004).

[11] L. Ruskó, G. Bekes, M. Fidrich, **"Automatic segmentation of the liver from multi- and single-phase contrast-enhanced CT images"**, *Med. Image Anal*., 13 (6) (2009) 871-882.

[12] A.H. Foruzan, R.A. Zoroofi, M. Hori, Y. Sato, **"A knowledge-based technique for liver segmentation in CT data"**, *Comp. Med. Imag. and Graph*., 33 (8) (2009) 567-587.

[13] S.J. Lim, Y.Y. Jeong, Y.S. Ho, **"Automatic liver segmentation for volume measurement in CT Images"**, *J. Vis. Commun. Image R.*, 17 (4) (2006) 860–875.

[14] L. Gao, D. Heath, B. Kuszyk, E. Fishman, **"Automatic liver segmentation technique for three-dimensional visualization of CT data"**, *Radiology*, 201 (1996) 359–364.

[15] F. Liu, B. Zhao, P. K. Kijewski, L. Wang, L. H. Schwartz, **"Liver segmentation for CT images using GVF snake"**, *Med. Phys*., 32 (12) (2005) 3699–3706.

[16] K.T. Bae, M.L. Giger, C.T. Chen, C. E. Kahn, **"Automatic segmentation of liver structure in CT images"**, *Med. Phys*., 20 (1) (1993) 71–78.

[17] E.L. Chen, P.C. Chung, C.L. Chen, H. M. Tsai, C.I. Chang, **"An automatic diagnostic system for CT liver image classification"**, *IEEE Trans. Med. Imag*., 22 (4) (2003) 483-492.

[18] J. Lee, N. Kim, H. Lee, J.B. Seo, H.J. Won, Y.M. Shin, Y.G. Shin, S.H. Kim, **"Efficient liver segmentation using a level-set method with optimal detection of**

the initial liver boundary from level-set speed images", *Comput. Meth. Prog. Biomed*., 88 (1) (2007) 26-38.

[19] Y. Zhao, Y. Zan, X. Wang, G. Li, **"Fuzzy C-means clustering-based multilayer perceptron neural network for liver CT images automatic segmentation"**, *in: Proceedings of Control and Decision Conference (CCDC)*, 2010, pp. 3423-3427.

[20] M. Pham, R. Susomboon, T. Disney,D. Raicu, J. Furst, **"A comparison of texture models for automatic liver segmentation"**, *in: Proceedings of the SPIE Medical Imaging 2007: Image Processing Conference*, San Diego, CA, USA , February 2007.

[21] S. Geman and D. Geman, **"Stochastic relaxation, gibbs distributions, and the bayesian restoration of images"**, *IEEE Trans. Pattern Anal. Mach. Intell.*, 6 (6) (1998) 721–741.

[22] N.H. Abdel-massieh, M.M. Hadhoud, K.A. Moustafa, **"A fully automatic and efficient technique for liver segmentation from abdominal CT images"**, *in: Proceedings of the 7th International Conference on Informatics and Systems*, May 2010, pp. 1-8.

[23] M. Kass, A.Witkin, D. Terzopolous, **"Snake: Active contour models"**, *Int. J. Comp. Vision*, 1 (4) (1987) 321-331.

[24] T. Chan, L.Vese, **"Active contours without edges"**, *IEEE Trans. Image Process*., 10 (2) (2001) 266–277.

[25] G. Chen, L. GU, **"A novel liver perfusion analysis based on active contours and chamfer matching"**, *Medical Imaging and Augmented Reality (Lecture Notes in Computer Science 4091),* Springer-Verlag, Berlin, Germany, 2006, pp.108–115.

[26] H. G. Barrow, J. M. Tenenbaum, R. C. Bolles, H. C. Wolf, **"Parametric correspondence and chamfer matching: Two new techniques for image matching",** , *in: Proceedings 5th Int. Joint Conf. Artif. Intell*, 1997, pp. 659– 663.

[27] G. Borgefors, **"Hierarchical chamfer matching: A parametric edge matching algorithm"**, *IEEE Trans. Pattern Anal. Mach. Intell*., 10 (6) (1988) 849–865.

[28] O. Gloger, J. Kühn, A. Stanski, H. Völzke, R. Puls, **"A fully automatic three-step liver segmentation method on LDA-based probability maps for multiple contrast MR images"**, *Magnetic Resonance Imaging*, 28 (16) (2010) 882-897.

[29] I. Middleton, R. Damper, **"Segmentation of magnetic resonance images using a combination of neural networks and active contour models"**, *Med. Eng. Phys*., 26 (1) (2004) 71-86.

[30] Li, B. and Acton, S.T. **"Active contour external force using vector field convolution for image segmentation"**. *IEEE Transactions on Image Processing* 16,pp: 2096-2106 ,2007

[31] R.C.Gonzalez and R.E. Woods. *Digital Image Processing*, 2nd. Ed.Prentice-Hall,2002

[32] J. Awad, T.K. Abdel-Galil, M.M.A. Salama, A. Fenster, K. Rizkalla, and D.B. Downey, **"Prostate's boundary detection in transrectal ultrasound images using scanning technique"**, *IEEE CCECE*,2003, pp: 1199–1202.

[33] Martin T.Hagan, Howard B.Dcmuth, *Mark Beale: Neural Network Design*, 2002.

[34] M. Kass, A. Witkin, and D. Terzopoulos, **"Snakes: Active contour models"**, *International Journal of Computer Vision*, vol. 1, no. 4, pp. 321-331, 1987

[35] Xu, Jerry L. Prince, **"Snakes, Shapes, and Gradient Vector Flow"**, *IEEE Trans. Image Processing*, 7 (36) (1998), pp: 359–369.

[36] D. Yuan and S. Lu, **"Simulated static electric field (SSEF) snake for deformable models"**, *in International Conference on Pattern Recognition*, Quebec, Canada, 2002.